A recyclable ionogel with high mechanical robustness based on covalent adaptable networks

Xiaotong Fan, Yifei Luo, Ke Li, Yi Jing Wong, Cong Wang, Jayven Chee Chuan Yeo, Gaoliang Yang, Jiaofu Li, Xian Jun Loh*, Zibiao Li*, and Xiaodong Chen*

Dr. X. Fan, Prof. Z. Li

Institute of Sustainability for Chemicals, Energy and Environment (ISCE²), Agency for Science, Technology and Research (A*STAR), 1 Pesek Road, Jurong Island, Singapore 627833, Republic of Singapore.

E-mail: lizb@imre.a-star.edu.sg

Dr. Y. Luo, Dr. K. Li, Y. J. Wong, Dr. J. C. C. Yeo, Dr. G. Yang, Prof. X. Loh, Prof. Z. Li Institute of Materials Research and Engineering (IMRE), Agency for Science, Technology and Research (A*STAR), 2 Fusionopolis Way, Singapore 138634, Republic of Singapore.

Y. J. Wong, Dr. C. Wang, Dr. J. Li, Prof. X. Chen

Innovative Center for Flexible Devices (iFLEX), Max Planck-NTU Joint Lab for Artificial Senses, School of Materials Science and Engineering, Nanyang Technological University, 50 Nanyang Avenue, Singapore 639798, Singapore

E-mail: chenxd@ntu.edu.sg

Prof. Z. Li

Department of Materials Science & Engineering, National University of Singapore, 9 Engineering Drive 1, Singapore 117575, Singapore

X. Fan and Y. Luo contributed equally to this work.

Keywords: Ionogels, closed-loop recyclability, covalent adaptable networks, strain sensors, human-machine interfaces

Abstract

Ionogels are an emerging class of soft materials for flexible electronics, with high ionic conductivity, low volatility, and mechanical stretchability. Recyclable ionogels are recently developed to address the sustainability crisis of current electronics, through the introduction of non-covalent bonds. However, this strategy sacrifices mechanical robustness and chemical stability, severely diminishing the potential for practical application. Here, covalent adaptable networks (CANs) are incorporated into ionogels, where dynamic covalent crosslinks endow high strength (11.3 MPa tensile strength), stretchability (2396% elongation at break), elasticity (energy loss coefficient of 0.055 at 100% strain), and durability (5000 cycles of 150% strain). The reversible nature of CANs allows the ionogel to be closed-loop recyclable for up to 10 times. Additionally, the ionogel is toughened by physical crosslinks between conducting ions and polymer networks, breaking the common dilemma in enhancing mechanical properties and electrical conductivity. The ionogel demonstrated robust strain sensing performance under harsh mechanical treatments and was applied for reconfigurable multimodal sensing based on its recyclability. This study provides insights into improving the mechanical and electrical properties of ionogels towards functionally reliable and environmentally sustainable bioelectronics.

1. Introduction

Ionogels are organic or inorganic networks dispersed in ionic liquids (ILs).^[1-3] Because of their ionic conductivity, mechanical flexibility, chemical, thermal, and electrochemical stability, low volatility, as well as rich design freedom, ionogels have attracted considerable attention and have been explored for various applications, such as bioelectronics, energy storage, sensors, and actuators.^[4-13] One of the promising applications is ionic skins, skin-conformal devices for sensing (*e.g.*, mechanical sensing,^[14-20] temperature sensing,^[21-22] chemical sensing^[23]), energy harvesting,^[24] and potentially other functions. These devices can be used for health monitoring, rehabilitation, athletic performance assessment, and human-machine interfaces.^[25-27]

The escalating environmental issues of current electronics^[28] motivate the development of environmentally sustainable ionogels. One way towards sustainable ionogels is to make the materials easily recyclable^[29] and self-healable. Noticeable research progress has been made in this direction by introducing non-covalent bonds into ionogel systems.^[30-34] For example, Yan's group^[31] fabricated recyclable ionogels employing hydrogen bonding and reversible entanglements. The ionogels could be recycled in water. Sun *et al.*^[33] fabricated thermochromic ionogels for antifogging windows with the properties of self-adhesiveness and self-healing. Owing to the presence of hydrogen bonds, the ionogels could be recycled by room-temperature pressing. Li and co-workers^[34] fabricated ultra-tough ionogels by the metal coordination interactions between halometallate ILs and polymer chains, which could be recycled in water.

Despite the successful demonstration of recyclability, the introduction of non-covalent bonds negatively impacts the mechanical robustness of ionogels, in terms of strength, stretchability, and toughness.^[35] It also gives rise to high hysteresis and property drifting upon cyclic loading due to large energy dissipation by physical crosslinks,^[36] diminishing device stability and precision. Additionally, non-covalent bonds can render ionogels susceptible to water or organic solvents at room temperature, further deteriorating their structural integrity and performance in complex environments, thereby limiting potential applications. Therefore, mechanical robustness (and chemical resistance) and recyclability (and self-healability) impose contradictory requirements in material design, which is a great challenge towards functionally reliable yet environmentally sustainable ionogels.^[31]

A promising strategy to tackle this issue is to incorporate covalent adaptable networks (CANs). CANs are polymer materials that can dynamically reconfigure their structure and properties in response to external stimuli, such as pH, light, or temperature, due to the presence of dynamic covalent bonds.^[37-40] While CANs can maintain stability under operating conditions, the polymer networks can be disrupted and rearranged upon change in environmental

conditions.^[41-45] The benefits of incorporating CANs into ionogels are twofold. First, the covalent nature of bonding inside CANs can enhance the mechanical robustness and solvent resistance of ionogels. Second, the stimuli-responsive breakage of dynamic covalent bonds can preserve recyclability and self-healability of ionogels. Consequently, CANs can help ionogels to maintain structural integrity during service with enhanced mechanical robustness, while still being recyclable and self-healable upon mild stimulation, expanding ionogels lifespan and broadening their applications.

Another major challenge facing ionogel design is the conflict between high electrical conductivity and strong mechanical properties (*e.g.*, high strength, large elongation, high toughness). The improvement of ionic conductivity is often achieved by increasing the content of ILs,^[2, 20, 46] but due to the reduction of polymer content, it usually leads to a decrease in mechanical properties. For example, Liu's group^[46] fabricated ionogels for biopotential monitoring. As the IL content increased from 10 wt% to 50 wt%, the conductivity increased gradually while Young's modulus decreased from 7.5 MPa to 4.5 MPa, and elongation at break decreased from 1500% to 620%. Another recent example is reported by Jia *et al.*,^[20] where they constructed polyrotaxane-based ionogels, whose tensile strength decreased from 130 kPa to 10 kPa and elongation at break decreased from 460% to 225% with the [BM][TFSI] content increasing from 25 wt% to 150 wt%. A possible solution to break this dilemma is to introduce interactions between conducting ions and polymer networks so that increasing the concentration of ions could simultaneously enhance the mechanical properties and electrical conductivity of ionogels.

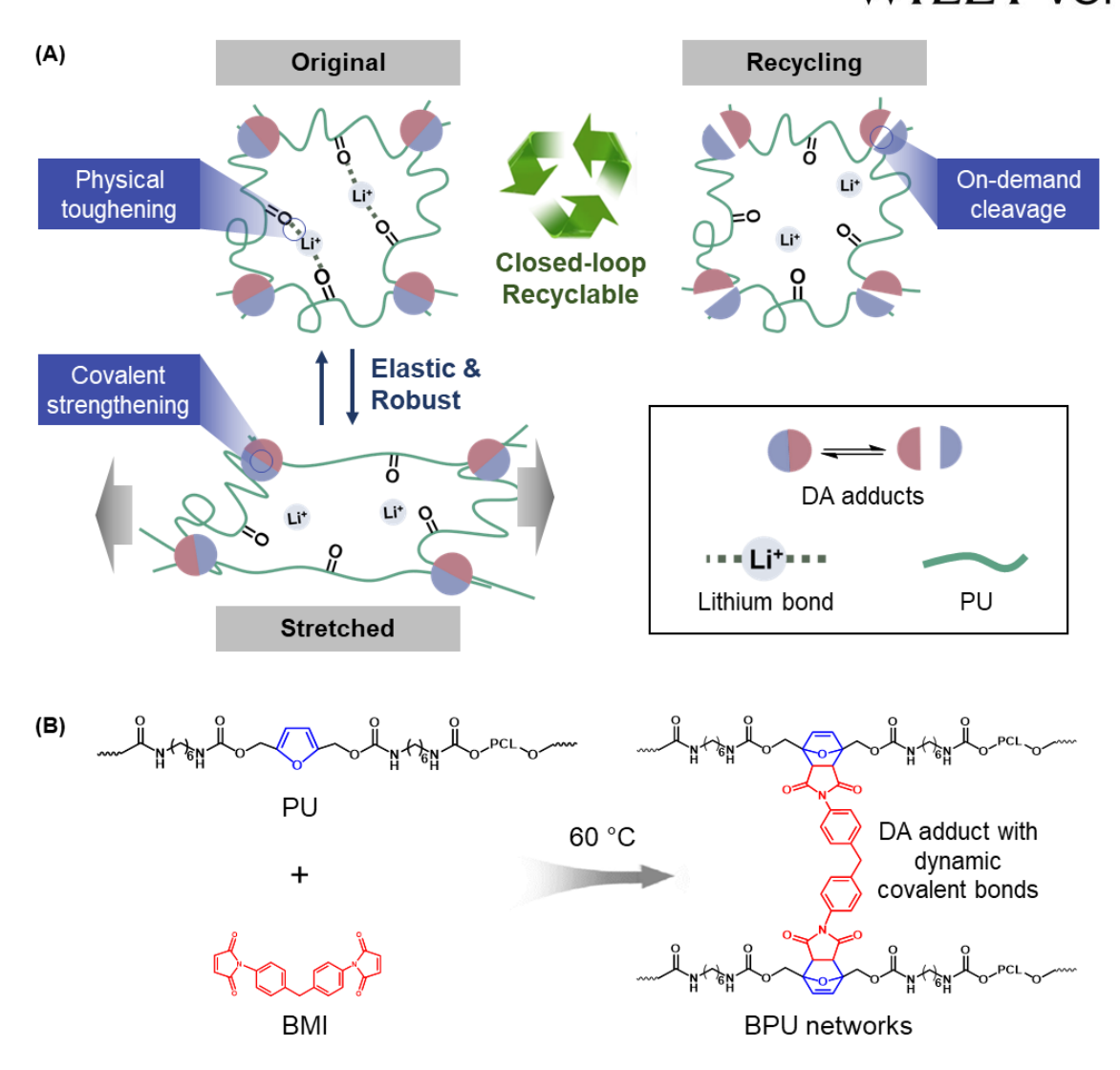


Figure 1. Design and preparation of the ionogel. (A) Schematic illustration of polymer network design for robust and recyclable ionogels. (B) Synthesis procedure of the dynamic covalent bonds crosslinked polyurethane chains.

Combining the benefits from CANs and polymer-ion interactions, herein, we fabricated a series of ionogels employing polyurethane (PU) elastomer as the backbone, Diels-Alder (DA) adducts [47-48] as the dynamic covalent crosslinks, and [EMIM][TFSI] and LiTFSI as the conductivity contributors (**Figure 1**). The covalent crosslinking through DA adducts helps to enhance the mechanical robustness of the ionogels while the dynamic nature of DA adducts enables ionogels to be closed-loop recyclable, self-healable, and reconfigurable through thermal treatment without any additional chemicals or catalysts. Furthermore, carbonyl oxygens on the polymer networks offer ion-dipole interactions with Li ions (known as lithium bonds), simultaneously enhancing both the mechanical properties and ionic conductivity. Through such rational design, we realized a stretchable, elastic, and durable ionogel with a tensile strength of 11.3 MPa, an elongation at break of 2396%, and an energy loss coefficient

 (η) of 0.055 at 100% tensile strain. It maintained stable mechanical properties over 5000 stretching cycles at a maximal strain of 150%. Additionally, it can resist degradation in water and organic solvents at room temperature yet can be recycled for up to 10 times with negligible change in properties. Such ionogels can not only function as wearable strain sensors to detect human motions and control robotic movements but also to realize reconfigurable multimodal long-term sports monitoring through recycling used ionogel into different shapes with uncompromised durability. The design strategy proposed in this work has a broader impact on optimizing the mechanical and electrical properties of ionogels for various applications. Importantly, recyclable ionogels pave the way for next-generation smart electronics with greater environmental sustainability.

2. Results and Discussion

2.1. Fabrication and chemical characterization of ionogels

The PU elastomer-based ionogels were prepared by mixing bismaleimide (BMI, crosslinker) with PU in the presence of [EMIM][TFSI] and LiTFSI. The ionogels were denoted as BPU_{y-z} (BPU, bismaleimide crosslinked polyurethane; y and z indicate the mass percentage of [EMIM][TFSI] and LiTFSI to that of BPU, respectively). After preparing the ionogels, Fourier Transform Infrared (FTIR) was employed to examine the formed ionogels. As shown in Figure 2A, the absorption peak at around 1725 cm⁻¹ was assigned to C=O groups on the PU chain. With the addition of BMI into the polyurethane solution, the absorption peak at 1776 cm⁻¹ ¹ ascribed to C=O groups on DA adducts emerged (Figure 2B),^[49] indicating CANs were successfully introduced into the networks. The peaks at 1356 cm⁻¹ and 1056 cm⁻¹ (shaded in Figure 2A) were respectively attributed to the stretching vibrations of S=O and S-N-S on [TFSI], [50] confirming the presence of ionic liquids within the ionogels. After LiTFSI was introduced into the ionogels with an increasing content, the absorption peak at 1725 cm⁻¹ attributed to C=O groups on PU chains weakened and gradually shifted to lower wavenumbers (Figure 2C and 2D), indicating the formation of lithium bonds between Li⁺ and C=O groups on PU chains. [51] Moreover, the characteristic peak at 1776 cm⁻¹ of DA adducts also experienced minor attenuation and redshift with increasing Li salt content (Figure S1), suggesting a possible interaction between Li⁺ and carbonyl oxygen on BMI crosslinkers. Density functional theory (DFT) calculations were further performed to give the possible conformations between lithium and C=O (Figure 2E and S2). Interaction Region Indicator (IRI)^[52] was employed to elucidate the complex structural interplay between lithium and C=O on the PU chain and BMI linkers. As delineated in Figure S2, the manifestation of the interaction between lithium and C=O was clearly discernible, providing theoretical evidence for lithium bond formation. One lithium

atom could bind two (Figure 2E, top), three, or four C=O groups on polyurethane chains. Moreover, one lithium atom could bind two C=O groups within one BMI molecule or from two different BMI molecules (Figure 2E, bottom). This observation by the IRI analysis is in accordance with FTIR results, confirming the formation of lithium bonds within the polymer network. Furthermore, the ionogels exhibited high transparency with light transmittance exceeding 96% (Figure S3), indicating excellent compatibility between polymer networks and ionic liquids.

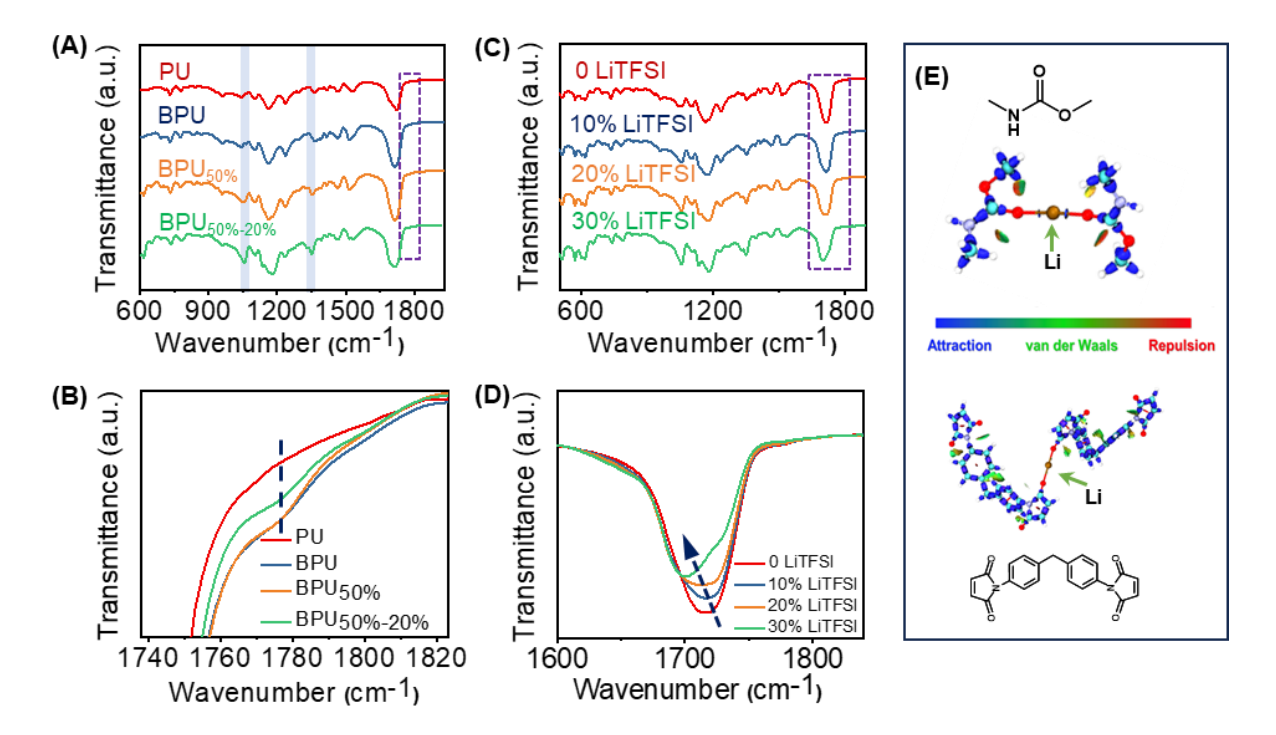


Figure 2. Chemical characterization and calculation to verify CANs and Li bonds formation. (A, B) FTIR spectra of PU, BPU, BPU_{50%} ionogel and BPU_{50%-20%} ionogel. (C, D) FTIR spectra of ionogels with various LiTFSI content. (E) The isosurface map of IRI=1.0 of representative conformations between Li⁺ and C=O on the PU chain segment (top), and C=O on BMI linkers (bottom). Oxygen in red, hydrogen in white, carbon in cyan, and nitrogen in light blue.

2.2. Mechanical properties of ionogels

The mechanical properties of ionogels at varying crosslinker, IL, and lithium salt contents were first systematically studied. As shown in Figure S4A, a higher crosslinker ratio resulted in higher tensile strength and shorter elongation at break, presumably due to higher crosslinking density. When crosslinker ratio (relative to PU backbone) was fixed, an increase in [EMIM][TFSI] content from 25 wt% to 100 wt% led to a decrease in tensile strength from 14.5 MPa to 3.2 MPa and a decrease in elongation at break from 2210% to 1590% (Figure S4B and

S4D), which can be attributed to the reduction of polymer matrix content. With the addition of LiTFSI into the ionogels, lithium bonds were formed, serving as additional physical crosslinks, which toughened the ionogels^[53-55] and enhanced both the tensile strength and elongation at break. As shown in Figure S4C and S4E, BPU_{75%} ionogel without LiTFSI had a tensile strength of 6.4 MPa and an elongation at break of 1740%. In contrast, BPU_{75%-30%} with 30 wt% LiTFSI showed significantly higher strength, reaching up to 11.3 MPa, along with an improved elongation at break of 2396%. As LiTFSI content continued to increase to 40 wt%, the tensile strength and elongation at break significantly decreased (Figure S5A). This can be attributed to the fact that beyond a saturation concentration of lithium salt, no more lithium bonds were formed. At this concentration, lithium salt acted as plasticizers, weakening the inter-chain interactions. In contrast, the conductivity increased with LiTFSI content increase (Figure S5B). This can be explained by the fact that ionic conductivity is typically proportional to the effective number of mobile ions. We also found that as the temperature increased from -20 °C to 60 °C, the conductivity increased accordingly, which was ascribed to the improved mobility of ions at higher temperatures (Figure S6). Dynamic Mechanical Analysis (DMA) curves showed that glass transition temperature (Tg) of the ionogels increased from -33.6 °C to -23.2 °C with the increase of LiTFSI content from 10 wt% to 30 wt% (Figure S7). This confirmed that the polymer chains were restricted in motion by the additional physical crosslinks.

To verify our design concept of CAN-strengthened and Li-toughened ionogels, we characterized the mechanical properties of a series of control samples without or with different types of crosslinks. As shown in **Figure 3**A and 3B, the tensile strength of PU_{75%} ionogels was around 1.26 MPa with an elongation at break of 850%. After crosslinking the PU chains by BMI, the tensile strength and elongation at break of BPU_{75%} ionogels were respectively improved to 6.4 MPa and 1750%, suggesting the significant strengthening effect from dynamic covalent bonds. With the addition of LiTFSI into the BPU_{75%-20%} ionogels, mechanical properties were further improved, as explained previously. In contrast, the PU_{75%-20%} ionogels (presumably crosslinked by lithium bonds only) were much weaker than all other samples, indicating the indispensable role of covalent bonding in strengthening the gel network. The above results highlight the importance of having both CANs and Li bonds within the ionogels for optimal mechanical strength and stretchability.

The ionogel design incorporating CANs and ion-polymer interactions brings about benefits in both mechanical and electrical properties. The comparison of tensile strength and elongation at break in Figure 3C shows that the ionogels fabricated in this study exhibited one of the best combinations of high strength and high stretchability compared to previously reported recyclable ionogels.^[30-31, 33-34, 56-58] Meanwhile, higher LiTFSI content resulted in an

elevation of ionic conductivity (Figure 3D). This contrasts with the deteriorating mechanical strength (Figure S4B) yet increasing conductivity (Figure S8) with the addition of ILs. The simultaneous improvement of ionic conductivity and mechanical performance broke a common dilemma in ionogels, where improved ionic conductivity usually resulted in a decline in mechanical strength. [59-61] Therefore, the strategy of incorporating physical interactions between the ionogel networks and conducting ions is a promising method for developing mechanically robust ionogels with good ionic conductivity. Demonstrating the mechanical capability of the ionogels, a 0.05 g ionogel film with a thickness of 0.2 mm and a width of 0.3 cm can effortlessly elevate an object weighing 1 kg (Figure 3E). In addition, the ionogel could withstand slicing even during substantial deformation (Figure 3F), making it highly advantageous for application in harsh mechanical environments.

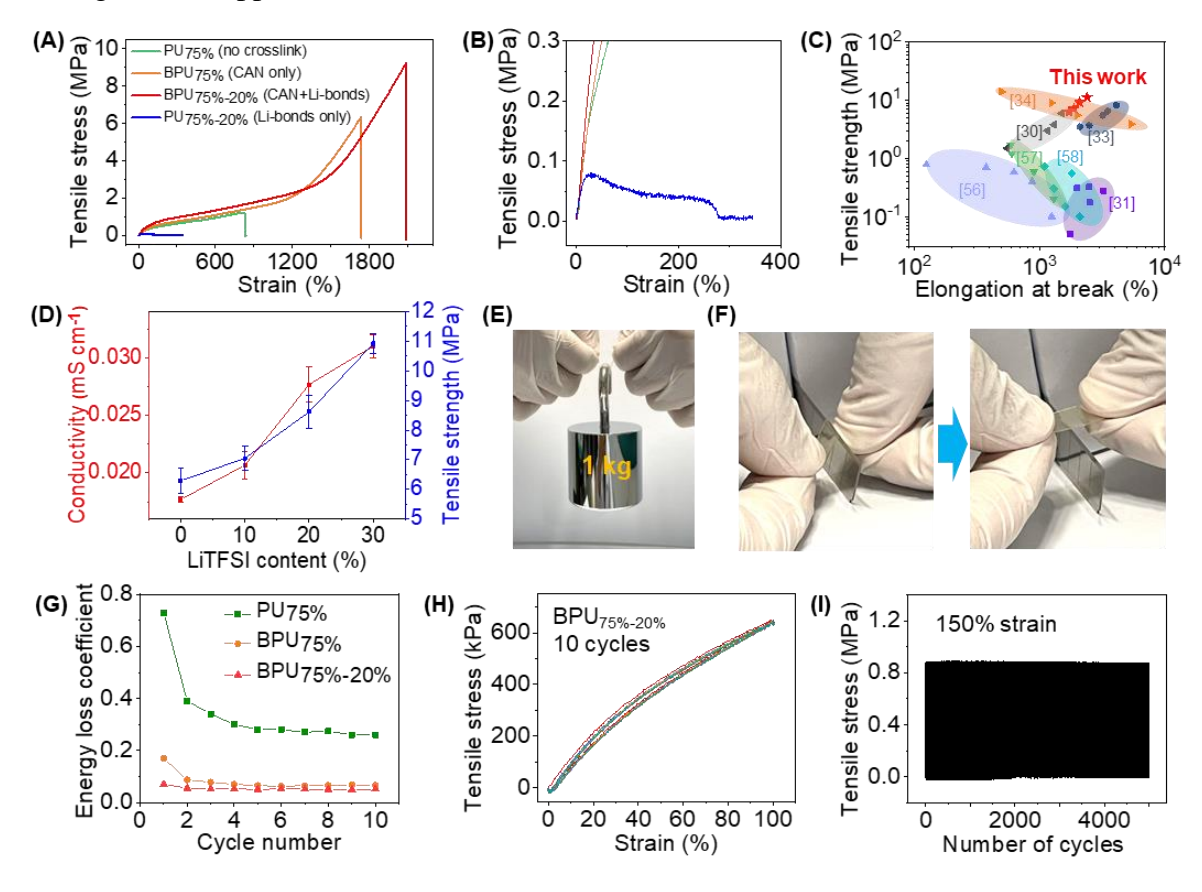


Figure 3. Mechanical robustness of the ionogel. Stress-strain curves of PU_{75%}, BPU_{75%}, BPU_{75%}, BPU_{75%}, BPU_{75%}, PU_{75%-20%} ionogels in the (A) whole range to 2400% and (B) the range to 400%. BPU: bismaleimide crosslinked polyurethane. BPU_{y-z}, y and z indicate the mass percentage of [EMIM][TFSI] and LiTFSI to that of DA adduct crosslinked polyurethane, respectively. (C) Comparison of tensile strength and elongation at break between this work and other recyclable ionogels. (D) Conductivity and tensile strength of ionogels with 75 wt% [EMIM][TFSI] and different LiTFSI content. (E) Picture of BPU_{75%-20%} lifting 1 kg weight. (F) Pictures indicating the BPU_{75%-20%} ionogel could withstand slicing even under substantial deformation. (G)

Comparison of the energy loss coefficient (η) of different ionogels for a strain of 100% during 10 cycle loading-unloading tests. (H) Stress-strain curves of BPU_{75%-20%} ionogel during ten cycles of tensile test at 100% strain. (I) Stress-strain curves of BPU_{75%-20%} ionogel under consecutive 5000 cycles at 150% strain.

Cyclic tensile test of BPU_{75%-20%} ionogels with varying strains from 100% to 600% was carried out (Figure S9). The loading-unloading curves of BPU_{75%-20%} presented no remarkable hysteresis compared to that of PU_{75%} and BPU_{75%} (Figure S10), indicating the best elasticity among the three ionogels. In addition, 10 consecutive tensile cycles at the strain of 100% were also performed for these three ionogels (Figure 3G, 3H, S10B and S10D). Except for the first cycle (energy loss coefficient, η =0.062) of BPU_{75%-20%}, each cycle remained stable with η of around 0.055, indicating outstanding elasticity and stability during stretching. In contrast, during the consecutive tensile cycles at a strain of 100%, the PU_{75%} ionogels without any crosslinking showed a η value ranging from 0.73 to 0.26. With the PU chains crosslinked by DA adducts, the elasticity of BPU_{75%} ionogels became better, exhibiting a η value ranging from 0.17 to 0.068. The best elasticity and stability of BPU_{75%-20%} ionogels among the three ionogel samples was presumably due to the crosslinked structure by dynamic covalent bonds and a minor contribution from lithium bonds. Figure 3H showed that BPU_{75%-20%} ionogels exhibited almost overlapping stress-strain curves with negligible residual strain during the 10 consecutive tensile cycles at the strain of 100%. Furthermore, BPU_{75%-20%} ionogels remained stable even during consecutive 5000 cycles of stretching under 150% strain (Figure 3I). The ionogels were also chemically stable in water and various organic solvents (Figure S11), although minor swelling was observed. Figure S12 showed that the mechanical properties of ionogels exposed to an open atmosphere for one week remained almost unchanged from the original. The consecutive 40 cycles of stretching at the strain of 100% were also performed at -20 °C and 60 °C (Figure S13). The ionogels could mainten stable mechanical properties at such extreme temperatures during the cyclic stretch. Thermogravimetric analysis (TGA) (Figure S14) indicated that the ionogel weight remains unchanged till 325 °C. In all, a covalently crosslinked network is crucial in achieving mechanical robustness and stability in various chemical and physical environments.

2.3. Closed-loop recyclability of ionogels

With the development of society, the problems of material waste and environmental pollution urgently require electronic materials to be recyclable.^[62-63] Owing to the presence of dynamic bonds, the developed ionogels could be closed-loop recycled and self-healed. The

ionogels could be recycled by firstly hot pressing at 110 °C and then incubating at 60 °C (**Figure 4**A). Another route to recycle the ionogels was to dissolve the ionogels at 110 °C in N, N-dimethylformamide (DMF). After casting the solution onto a silicon mould and incubating it at 60 °C, the recycled ionogel can be obtained. These two straightforward one-pot closed-loop recycling approaches could theoretically endow ionogels with an endless lifecycle.

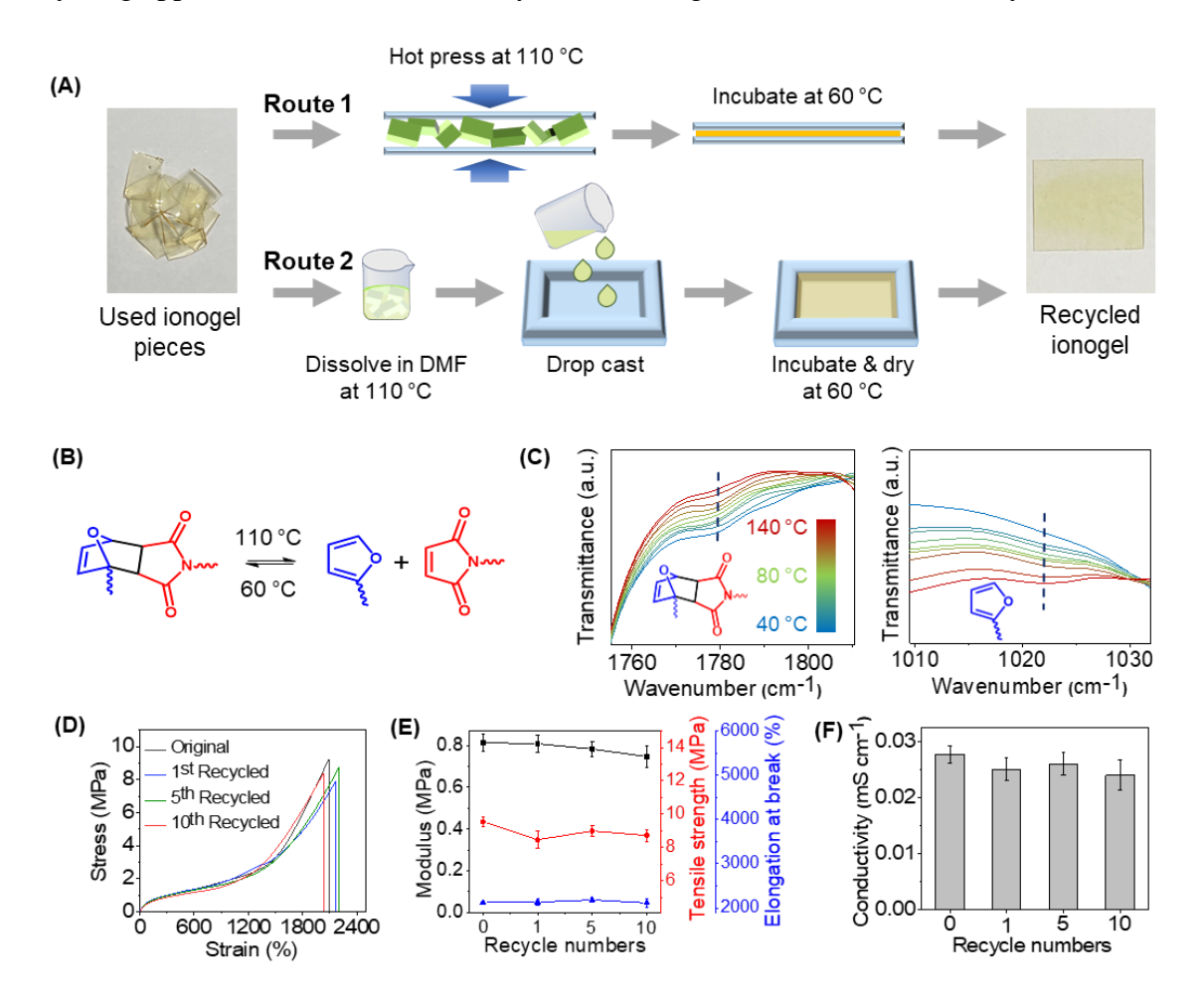


Figure 4. Recyclability of the ionogel. (A) The closed-loop recyclable process of the ionogels. (B) The reversible nature of DA reaction. (C) FTIR spectra of ionogels were recorded at real temperatures ranging from 40 °C to 140 °C. (D) The stress-strain curves of the BPU_{75%-20%} ionogels at different recyclable cycles by DMF solvent method. (E) Comparing the tensile properties of BPU_{75%-20%} ionogel at different recyclable cycles by DMF solvent method. (F) The conductivity of BPU_{75%-20%} ionogel after being recycled for different times by DMF solution method.

The chemistry basis for recycling was next investigated. Theoretically, furan undergoes a reaction with maleimide to produce a DA adduct under low-temperature conditions (Figure 4B). At elevated temperatures, the retro-DA reaction takes place.^[47-48] This inherent dynamic

nature of DA reaction allows ionogels to exhibit one-pot closed-loop recyclability. The reactions were experimentally examined by real-temperature FTIR. As shown in Figure 4C, the absorption peak at 1776 cm⁻¹ corresponding to DA adducts experienced obvious weakening as the temperature increased above 110 °C, and the peak at 1022 cm⁻¹ assigned to the furan ring gradually became more prominent at a temperature above ~100 °C. These results pointed to the cleavage of DA adducts into maleimide and furan with an increase in temperature. Moreover, the ionogels heated at 60 °C in DMF could not be dissolved because of the undissociated state of DA adducts at this temperature (Figure S15), further confirming the temperature requirement for the retro-DA reaction. Gel contents of DA adducts crosslinked PU were also calculated using various common organic solvents, which are all larger than 91% (Figure S16). This indicated the formation of highly crosslinked polymer networks. As temperature increased, the C=O absorption peak slightly weakened in intensity without obvious wavenumber shift, suggesting lithium bonds were almost not affected by temperature (Figure S17).^[51] We demonstrated the closed-loop recyclability of the ionogels by recycling BPU_{75%-20%} for 10 times. The unchanging characteristic peaks in FTIR spectra (Figure S18) suggested that the structure of the recycled ionogels remained almost unchanged compared to the original, even after 10 recycling cycles using either DMF solvent or the hot-pressing method. Scanning electron microscopy (SEM) was used to observe the inner structures of the ionogels before and after the recycling process. Homogenous and interconnected network structures can be observed in the original samples (Figure S19A and S19B). After recycling by DMF solvent or hot-pressing method, we could still observe similar interconnected and continuous structures (Figure S19C-S19F), indicating that the recycling process did not affect the inner structures of the ionogels. Thanks to the retention of the ionogel structure, the mechanical characteristics of the ionogels, including tensile strength, elongation at break, and Young's modulus, displayed almost no alterations compared to the original samples (Figure 4D, 4E, S20A, S20B). The conductivity test of the ionogels after 10 cycles also yielded data similar to the original results (Figure 4F and S20C). Additionally, T_g of the BPU_{75%-20%} sample, as determined through DMA analysis, exhibited negligible change after recycling (Figure S21). Furthermore, both the original and recycled ionogels can be integrated into circuits and light up a light-emitting diode (LED) when powered (Figure S22). In addition, the ionogels were still transparent after being recycled (Figure S23).

Due to the temperature-sensitive nature of the DA reaction, the cut ionogels can be self-healed by heating at 110 °C to cleave the DA adducts, followed by incubation at 60 °C to ensure the complete association between furan and maleimide groups (Figure S24A). The stress-strain curve of the self-healed ionogel was almost the same as that of the original ionogel (Figure

S24B and S25), indicating good self-healing ability. In contrast, the ionogel failed to heal after only incubation at 60 °C for 24 h because the DA adducts did not dissociate at 60 °C, and lithium bonds alone could not facilitate the self-healing (Figure S24C). The dynamic nature of the DA adducts also made the ionogels reconfigurable between different shapes (Figure S26). These results demonstrate that CANs confer one-step closed-loop recyclability as well as self-healing ability and reconfigurability to ionogels without adverse impact on mechanical and electrical properties.

In practical applications, the choice of recycling method depends on specific needs. If thin and flat samples are required, the hot-pressing method should be preferred because it can produce very flat samples, and the thickness can be adjusted by varying the pressure during hot pressing. If samples with special shapes are required, the DMF solvent method can be selected. By customizing molds of special shapes, ionogels with different shapes can be obtained through the DMF solvent method. The recycling methods for the reported recyclable ionogels are shown in Table S1. These ionogels can only be recycled by one method, either the solvent method or the pressing method, which limits recycling options. In contrast, our ionogels can be recycled by both the solvent method and the hot-pressing method. This flexibility allows the recycling method to be chosen based on specific needs and environmental constraints.

2.4. Robust and reconfigurable strain sensing applications

Tapping the ionic conductivity and mechanical stretchability of the developed ionogel, we utilized it as a stretchable strain sensor. First, we visualized the strain-sensitive resistance of the ionogel by connecting it with an LED and a power source. The LED could be lighted up and dimmed significantly when the ionogel strip was stretched (Figure S27), indicating substantial resistance change with strain (detailed analysis of sensing mechanism found in Supporting Note 1, Supporting Information). We then quantitatively characterized the strain sensing performance of the ionogel by measuring the relative resistance change, expressed as $\Delta R/R_0 = (R-R_0)/R_0$ where R_0 is the original resistance without strain and R is the resistance in response to a certain strain. We also calculated its gauge factor (GF) defined as $GF = (\Delta R/R_0)/(\Delta L/L_0)$ where L_0 is the original sample length and ΔL is the change in length due to stretch. Figure S28A showed $\Delta R/R_0$ had a two-stage linear relationship with strain, with a GF of 0.79 for strain below ~40% ($R^2 = 0.998$) and a GF of 1.2 for strain above ~40% ($R^2 = 0.999$). The response time and recovery time was found to be 94 ms and 68 ms respectively (Figure S29), comparable or superior to previous reports. During consecutive cycles of extension and relaxation with tensile strains ranging from 10% to 100% (Figure S28B), the

ionogel generated reversible and reproducible $\Delta R/R_0$ signals. Furthermore, the ionogel demonstrated stable resistance change during 2000 consecutive loading-unloading cycles at 100% maximum strain (Figure S28C), which was among the best in terms of durability even when compared with non-recyclable ionogel-based strain sensors (Table S2). Such superior mechanical and electrical durability should be attributed to the chemically crosslinked polymer networks as well as the ion-dipole interactions^[51, 66] between conducting ions and the polymer matrix.

The ionogels could be used as wearable sensing devices for monitoring various human body motions, including finger bending at different degrees (Figure S28D), wrist bending (Figure S28E), as well as large-range elbow bending (Figure S28F). The developed ionogels could also monitor and differentiate the fast and slow bending of two fingers (Figure S28G). More importantly, ionogels recycled by hot-pressing or DMF solvent method still showed comparable sensing performance to the original ionogels (Figure S28H and S28I). We noticed that the sensitivity and stability of the ionogel strain sensor experienced a slight decrease at 60 °C (Figure S30), which might be caused by the enhanced mobility of PCL segments in the PU network.^[67]

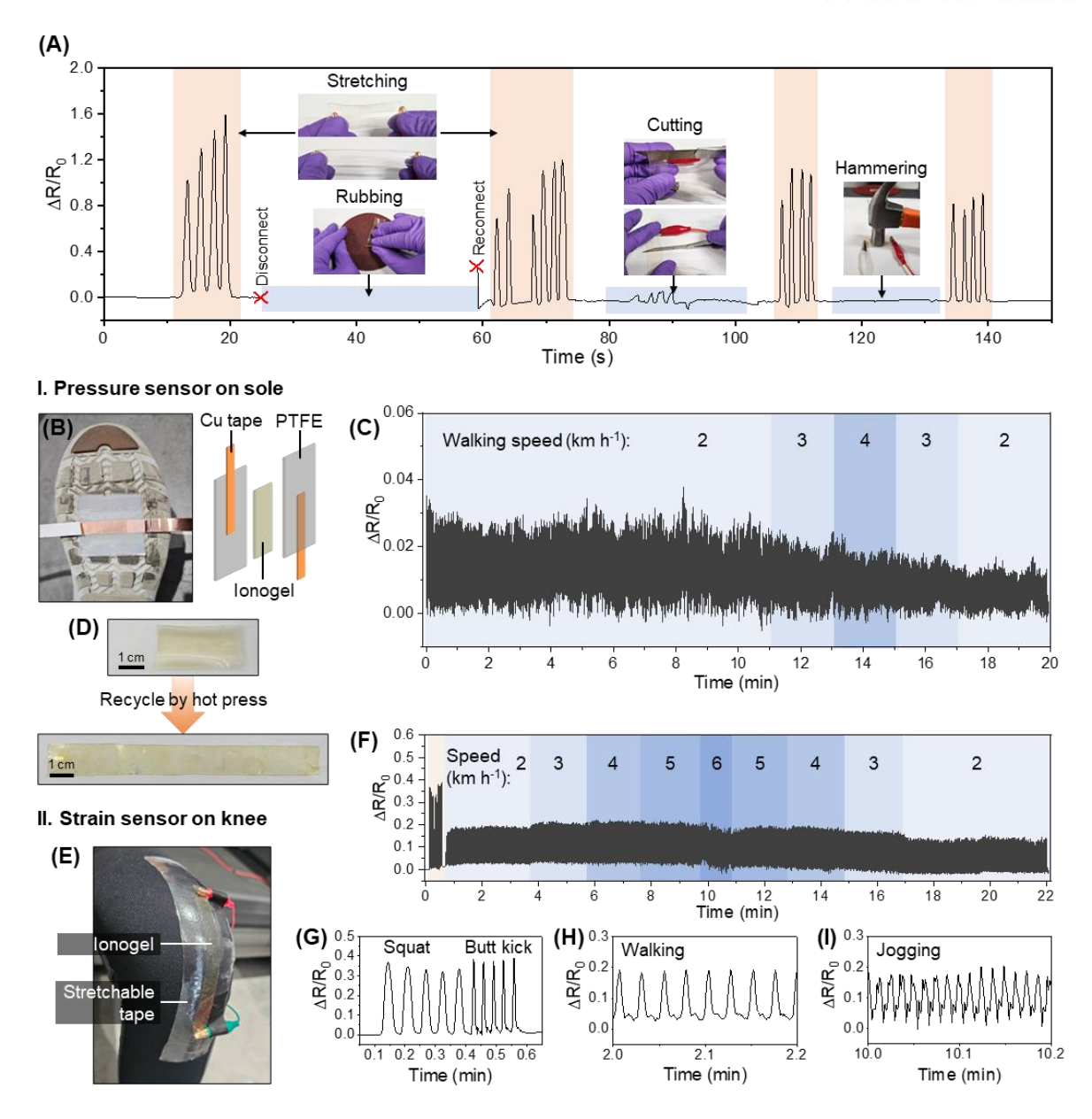


Figure 5. Damage-tolerant strain sensing and changeable modes of long-term sports monitoring enabled by the robust and recyclable ionogel. (A) Relative resistance change of a piece of ionogel upon manual stretching and experiencing rubbing against sandpaper, cutting, and hammering, showing the unaffected strain-responsiveness. (B) Photograph of an ionogel-based pressure sensor on sole (left) and schematic of the pressure sensor (right). PTFE, poly(tetrafluoroethylene). (C) Relative resistance change of the pressure sensor during walking on a treadmill at varying speed. (D) Photographs of ionogel used in the pressure sensor and after recycling into a new shape for strain sensing. (E) Photograph of ionogel-based strain sensor attached on knee. (F) Relative resistance change of the strain sensor during various exercises (zoom-in view in (G) to (I)), showing the durability against repetitive stretching even after recycling.

To demonstrate the mechanical robustness of the ionogel, we rubbed, cut, and hammered an ionogel piece while monitoring its resistance change with stretching (**Figure 5**A, Video S1). Even under such extreme mechanical treatments, the strain-sensing performance was not compromised. Furthermore, when an ionogel-based pressure sensor was attached to a sole (Figure 5B), it could monitor walking for at least 20 minutes (~1000 pressing cycles, Figure 5C, Video S2), and individual steps were distinguishable in the output signal for calculation of stepping speed (Figure S31). The attenuating resistance responses after ~10 min (Figure 5C) likely originates from the stiffening of the ionogel upon cyclic compression, which is consistent with our compression test (Figure S32). Thanks to the recyclability of the ionogel, it was then reconfigured by hot pressing into a new shape for strain sensing (Figure 5D). The strain sensor made from the recycled ionogel was attached to the knee for exercise monitoring (Figure 5E). Though recycled, it still had good durability to continuously function for at least 22 minutes (~1200 stretching cycles) with stable resistance output (Figure 5F, Video S3) and was capable of different exercise tracking (Figure 5G-5I). The above results demonstrate the mechanical robustness, durability, and unique advantages brought about by the recyclability of the developed ionogel. We further demonstrated the application of human motion sensing for remotely controlling the movement of a robot (Figure S33). Finger motions were captured by ionogel-based strain sensors, and sensor signals were transmitted to a laptop and analyzed by a self-developed user interface on MATLAB. Once the strain sensor output reached a threshold, a command was sent through Bluetooth to the microcontroller of the robot, which triggered the desired motion. Figure S33D and Video S4 showed that upon finger bending, the robot could move according to the preprogrammed walking route. In addition, the ionogel does not cause skin irritation (Figure S34), demonstrating its compatibility with human skin and safety to use as a wearable strain sensor.

The proposed strategy of fabricating recyclable ionogels by incorporating CANs into polymer networks can be extended to other ILs and CANs. Other dynamic covalent bonds, such as disulfide bonds, imine bonds, or boronic ester bonds can also be selected for preparing recyclable ionogels. However, when selecting other dynamic covalent bonds, we should make a rational design for dynamically crosslinked polymer networks and consider the recycling complexity. Other dynamic covalent bonds usually require catalysts to be cleaved, such as reducing agents for disulfide bonds, and acids for imine bonds. The introduction of catalysts may complicate the recycling process and increase costs. As for the selection of ILs, ILs with lower viscosity and smaller anion size should be considered for higher conductivity. Furthermore, high compatibility between ILs and polymer networks is essential for good mechanical properties and uniformity of ionogels.

3. Conclusion

In summary, CANs were incorporated into ionogels to satisfy the contradictory requirements for mechanical robustness and recyclability. We fabricated ionogels by crosslinking polyurethane backbones through Diels-Alder (DA) reaction in the presence of [EMIM][TFSI] and LiTFSI. The dynamic covalent bonds on DA adducts endow ionogels with closed-loop recyclability up to 10 times as well as durability, stability, stretchability, and elasticity. By rational design of the polymer networks, lithium bonds are formed between lithium ions and carbonyl oxygens within polymer networks, simultaneously enhancing the mechanical toughness and electrical conductivity of the ionogels. For application, wearable strain sensors based on ionogels can be used for human motion detection and human-machine interfacing to control the movement of robots. The recyclability can be tapped for reconfigurable multimodal sports monitoring. This research offers a strategy for producing closed-loop recyclable and functionally durable ionogels, advancing the field of sustainable and eco-friendly bioelectronics.

4. Experimental Section/Methods

Experimental details are provided in Supporting Information. The tests on human skin were approved by Institute of Review Board, Nanyang Technological University (approval number: IRB-2017-08-035). All research participants provided consent for their data to be published in this manuscript.

Supporting Information

Supporting Information is available from the Wiley Online Library or from the author.

Acknowledgements

X. Fan and Y. Luo contributed equally to this work. The authors would like to acknowledge the financial support from the Agency for Science, Technology and Research (A*STAR) under its RIE2025 Manufacturing, Trade and Connectivity (MTC) Programmatic Funding (Grant No. M22K9b0049 and M23L8b0049).

References

- [1] L. C. Tome, L. Porcarelli, J. E. Bara, M. Forsyth, D. Mecerreyes, *Mater. Horiz.* **2021**, 8, 3239-3265.
- [2] X. Fan, S. Liu, Z. Jia, J. J. Koh, J. C. C. Yeo, C.-G. Wang, N. E. Surat'man, X. J. Loh, J. Le Bideau, C. He, Z. Li, T.-P. Loh, *Chem. Soc. Rev.* **2023**, *52*, 2497-2527.

- [3] M. Wang, P. Zhang, M. Shamsi, J. L. Thelen, W. Qian, V. K. Truong, J. Ma, J. Hu, M. D. Dickey, *Nat. Mater.* **2022**, *21*, 359-365.
- [4] A. Vioux, B. Coasne, Adv. Energy Mater. 2017, 7, 1700883.
- [5] J. Saez, T. Glennon, M. Czugala, A. Tudor, J. Ducree, D. Diamond, L. Florea, F. Benito-Lopez, *Sens. Actuators B Chem.* **2018**, 257, 963-970.
- [6] W. J. Hyun, C. M. Thomas, M. C. Hersam, Adv. Energy Mater. 2020, 10, 2002135.
- [7] T. Li, Y. Wang, S. Li, X. Liu, J. Sun, *Adv. Mater.* **2020**, *32*, e2002706.
- [8] H. Li, L. Li, J. Wei, T. Chen, P. Wei, *Small* **2023**, e2305848.
- [9] D. Lv, X. Li, X. Huang, C. Cao, L. Ai, X. Wang, S. K. Ravi, X. Yao, *Adv. Mater.* **2023**, e2309821.
- [10] M. Zhang, X. Tao, R. Yu, Y. He, X. Li, X. Chen, W. Huang, J. Mater. Chem. A 2022, 10, 12005-12015.
- [11] Y. Zhu, X. Li, Z. Zhao, Y. Liang, L. Wang, Y. Liu, Gels 2022, 8, 797.
- [12] G. Ge, Y. Zhang, X. Xiao, Y. Gong, C. Liu, C. Lyu, W. L. Ong, G. W. Ho, Z. Yang, W. Huang, *Adv. Funct. Mater.* **2024**, *34*, 2310963.
- [13] M. Wang, X. Xiao, S. Siddika, M. Shamsi, E. Frey, W. Qian, W. Bai, B. T. O'Connor, M. D. Dickey, *Nature* **2024**, 1-6.
- [14] X. Yu, Y. Zheng, Y. Wang, H. Zhang, H. Song, Z. Li, X. Fan, T. Liu, *Chem. Mater.* **2022**, *34*, 1110-1120.
- [15] K. G. Cho, S. An, D. H. Cho, J. H. Kim, J. Nam, M. Kim, K. H. Lee, *Adv. Funct. Mater.* **2021**, *31*, 2102386.
- [16] L. Sun, S. Chen, Y. Guo, J. Song, L. Zhang, L. Xiao, Q. Guan, Z. You, *Nano Energy* **2019**, *63*, 103847.
- [17] J. Zhang, E. Liu, S. Hao, X. Yang, T. Li, C. Lou, M. Run, H. Song, *Chem. Eng. J.* **2022**, *431*, 133949.
- [18] X. Zhao, J. Xu, J. Zhang, M. Guo, Z. Wu, Y. Li, C. Xu, H. Yin, X. Wang, *Mater. Horiz.* **2023**, *10*, 646-656.
- [19] S. Wu, J. Huang, S. Jing, H. Xie, S. Zhou, Adv. Funct. Mater. 2023, 33, 2303292.
- [20] R. Du, T. Bao, T. Zhu, J. Zhang, X. Huang, Q. Jin, M. Xin, L. Pan, Q. Zhang, X. Jia, *Adv. Funct. Mater.* **2023**, *33*, 2212888.
- [21] Z.-J. Chen, Y.-Q. Sun, X. Xiao, H.-Q. Wang, M.-H. Zhang, F.-Z. Wang, J.-C. Lai, D.-S. Zhang, L.-J. Pan, C.-H. Li, *J. Mater. Chem. A* **2023**, *11*, 8359-8367.
- [22] J. Wang, Y. Zheng, T. Cui, T. Huang, H. Liu, J. Zhu, L. Song, Y. Hu, *Adv. Funct. Mater.* **2023**, 2312383.
- [23] H. H. Chouhdry, D. H. Lee, A. Bag, N. E. Lee, *Nat. Commun.* **2023**, *14*, 821.
- [24] W. Liao, X. Liu, Y. Li, X. Xu, J. Jiang, S. Lu, D. Bao, Z. Wen, X. Sun, *Nano Res.* **2021**, *15*, 2060-2068.
- [25] L. Luo, Z. Wu, Q. Ding, H. Wang, Y. Luo, J. Yu, H. Guo, K. Tao, S. Zhang, F. Huo, J. Wu, *ACS Nano* **2024**, *18*, 15754-15768.
- [26] W. Wang, D. Yao, H. Wang, Q. Ding, Y. Luo, H. Ding, J. Yu, H. Zhang, K. Tao, S. Zhang, F. Huo, J. Wu, *Adv. Funct. Mater.* **2024**, 2316339.
- [27] J. Li, Q. Ding, H. Wang, Z. Wu, X. Gui, C. Li, N. Hu, K. Tao, J. Wu, *Nano-Micro Letters* **2023**, *15*, 105.
- [28] L. Lan, J. Ping, J. Xiong, Y. Ying, *Adv Sci (Weinh)* **2022**, *9*, e2200560.
- [29] E. A. Olivetti, J. M. Cullen, *Science* **2018**, *360*, 1396-1398.
- [30] H. Zhang, X. Yu, Y. Wang, X. Fan, Y.-E. Miao, X. Zhang, T. Liu, *Compos. Sci. Technol.* **2022**, *230*, 109740.
- [31] W. Li, L. Li, S. Zheng, Z. Liu, X. Zou, Z. Sun, J. Guo, F. Yan, *Adv. Mater.* **2022**, *34*, 2203049.
- [32] P. Liu, D. Pei, Y. Wu, M. Li, X. Zhao, C. Li, *J. Mater. Chem. A* **2022**, *10*, 25602-25610.
- [33] B. Li, F. Xu, T. Guan, Y. Li, J. Sun, Adv. Mater. 2023, 35, 2211456.

- [34] L. Li, W. Li, X. Wang, X. Zou, S. Zheng, Z. Liu, Q. Li, Q. Xia, F. Yan, *Angew. Chem. Int. Ed.* **2022**, *61*, e202212512.
- [35] C. Ma, J. Wei, Y. Zhang, X. Chen, C. Liu, S. Diao, Y. Gao, K. Matyjaszewski, H. Liu, *Adv. Funct. Mater.* **2023**, *33*, 2211771.
- [36] J. Y. Sun, X. Zhao, W. R. Illeperuma, O. Chaudhuri, K. H. Oh, D. J. Mooney, J. J. Vlassak, Z. Suo, *Nature* **2012**, *489*, 133-136.
- [37] N. Zheng, Y. Xu, Q. Zhao, T. Xie, Chem. Rev. 2021, 121, 1716-1745.
- [38] W. Zou, B. Jin, Y. Wu, H. Song, Y. Luo, F. Huang, J. Qian, Q. Zhao, T. Xie, *Sci. Adv.* **2020**, *6*, eaaz2362.
- [39] J. Zheng, Z. M. Png, S. H. Ng, G. X. Tham, E. Ye, S. S. Goh, X. J. Loh, Z. Li, *Mater. Today* **2021**, *51*, 586-625.
- [40] M. Podgórski, B. D. Fairbanks, B. E. Kirkpatrick, M. McBride, A. Martinez, A. Dobson, N. J. Bongiardina, C. N. Bowman, *Adv. Mater.* **2020**, *32*, 1906876.
- [41] G. M. Scheutz, J. J. Lessard, M. B. Sims, B. S. Sumerlin, *J. Am. Chem. Soc.* **2019**, *141*, 16181-16196.
- [42] C. J. Kloxin, C. N. Bowman, Chem. Soc. Rev. 2013, 42, 7161-7173.
- [43] Z. Tang, X. Lyu, A. Xiao, Z. Shen, X. Fan, Chem. Mater. 2018, 30, 7752-7759.
- [44] J. Smith-Jones, N. Ballinger, N. Sadaba, X. L. de Pariza, Y. Yao, S. L. Craig, H. Sardon, A. Nelson, *RSC Appl. Polym.* **2024**, *2*, 434-443.
- [45] H. Li, X. Wu, M. Li, P. Chen, J. Zhang, Z. Wang, Z. Wang, *Chem. Eng. J.* **2023**, *470*, 144263.
- [46] T. Chen, G. Ye, H. Wu, S. Qi, G. Ma, Y. Zhang, Y. Zhao, J. Zhu, X. Gu, N. Liu, *Adv. Funct. Mater.* **2022**, *32*, 2206424.
- [47] K. Jin, S.-s. Kim, J. Xu, F. S. Bates, C. J. Ellison, *ACS Macro Lett.* **2018**, 7, 1339-1345.
- [48] S. Wang, N. Wang, D. Kai, B. Li, J. Wu, J. C. C. Yeo, X. Xu, J. Zhu, X. J. Loh, N. Hadjichristidis, *Nat Commun.* **2023**, *14*, 1182.
- [49] X. Kuang, S. Wu, Q. Ze, L. Yue, Y. Jin, S. M. Montgomery, F. Yang, H. J. Qi, R. Zhao, *Adv. Mater.* **2021**, *33*, 2102113.
- [50] Z. Wang, Y. Si, C. Zhao, D. Yu, W. Wang, G. Sun, *ACS Appl. Mater. Interfaces.* **2019**, *11*, 27200-27209.
- [51] M. Zhang, R. Yu, X. Tao, Y. He, X. Li, F. Tian, X. Chen, W. Huang, *Adv. Funct. Mater.* **2022**, *33*, 2208083.
- [52] T. Lu, Q. Chen, Chem. Methods. 2021, 1, 231-239.
- [53] H. Park, T. Kang, H. Kim, J.-C. Kim, Z. Bao, J. Kang, *Nat Commun.* **2023**, *14*, 5026.
- [54] J. Kang, D. Son, G. J. N. Wang, Y. Liu, J. Lopez, Y. Kim, J. Y. Oh, T. Katsumata, J. Mun, Y. Lee, *Adv. Mater.* **2018**, *30*, 1706846.
- [55] J.-Y. Sun, X. Zhao, W. R. Illeperuma, O. Chaudhuri, K. H. Oh, D. J. Mooney, J. J. Vlassak, Z. Suo, *Nature* **2012**, *489*, 133-136.
- [56] C. Dang, C. Shao, H. Liu, Y. Chen, H. Qi, *Nano Energy* **2021**, *90*, 106619.
- [57] L. Sun, H. Huang, L. Zhang, R. E. Neisiany, X. Ma, H. Tan, Z. You, *Adv. Sci.* **2023**, 2305697.
- [58] L. Xu, Z. Huang, Z. Deng, Z. Du, T. L. Sun, Z. H. Guo, K. Yue, *Adv. Mater.* **2021**, *33*, 2105306.
- [59] S. Peng, Q. Guo, N. Thirunavukkarasu, Y. Zheng, Z. Wang, L. Zheng, L. Wu, Z. Weng, *Chem. Eng. J.* **2022**, *439*, 135593.
- [60] S. Wang, H. Cheng, B. Yao, H. He, L. Zhang, S. Yue, Z. Wang, J. Ouyang, *ACS Appl. Mater. Interfaces.* **2021**, *13*, 20735-20745.
- [61] Y. Fang, H. Cheng, H. He, S. Wang, J. Li, S. Yue, L. Zhang, Z. Du, J. Ouyang, *Adv. Funct. Mater.* **2020**, *30*, 2004699.
- [62] J. A. Chiong, H. Tran, Y. Lin, Y. Zheng, Z. Bao, Adv. Sci. 2021, 8, 2101233.
- [63] Z. Zhao, K. Xia, Y. Hou, Q. Zhang, Z. Ye, J. Lu, Chem. Soc. Rev. 2021, 50, 12702-12743.

- [64] Z. Yu, P. Wu, Adv. Mater. 2021, 33, e2008479.
- [65] J. Tie, Z. Mao, L. Zhang, Y. Zhong, H. Xu, Adv. Funct. Mater. 2023, 2307367.
- [66] L. Peng, L. Hou, P. Wu, Adv. Mater. 2023, 35, 2211342.
- [67] M. Bartnikowski, T. R. Dargaville, S. Ivanovski, D. W. Hutmacher, *Prog. Polym. Sci.* **2019**, *96*, 1-20.

The table of contents entry

The contradictory requirements of recyclability and robustness of ionogels are resolved by incorporating covalent adaptable networks (CANs), resulting in a closed-loop recyclable, elastic, tough, durable, and solvent-resistant ionogel. This ionogel demonstrates robust strain

sensing performance under harsh mechanical conditions and is applied for reconfigurable multimodal sensing due to its recyclability.

Xiaotong Fan, Yifei Luo, Ke Li, Yi Jing Wong, Cong Wang, Jayven Chee Chuan Yeo, Gaoliang Yang, Jiaofu Li, Xian Jun Loh*, Zibiao Li*, and Xiaodong Chen*

A recyclable ionogel with high mechanical robustness based on covalent adaptive networks

